

# Heat pipe collectors with overheating prevention in a cost-optimized system concept: Monitoring of system performance and stagnation loads under real conditions

Bert Schiebler<sup>a,\*</sup>, Jan Köhler<sup>b</sup>, Lukas Wagner<sup>a</sup>, Julian Jensen<sup>a</sup>, Federico Giovannetti<sup>a</sup>

<sup>a</sup> Institut für Solarenergieforschung Hameln (ISFH), Am Ohrberg 1, 31860 Emmerthal Germany

<sup>b</sup> AKOTEC Produktionsgesellschaft mbH, Grundmühlenweg 3, 16278 Angermünde Germany

## ARTICLE INFO

This paper was submitted and presented at EuroSun 2022 - the ISES and IEA SHC International Conference on Solar Energy for Buildings and Industry

### Keywords:

Solar thermal systems  
Heat pipe  
Stagnation load  
Overheating prevention  
Cost reduction  
LCoH

## ABSTRACT

Heat pipe collectors can significantly reduce stagnation loads in solar thermal systems due to their thermophysical properties. The paper experimentally investigates a novel system concept based on both evacuated tube collectors and flat-plate collectors with overheating prevention. Due to the resulting temperature limitation in the collector, the use of polymeric pipes as well as a significantly downsized expansion volume is possible. We implemented this concept in five demonstration plants and monitored their behavior over more than one year of operation. Both domestic hot water systems and combi-systems with space heating support in residential and office buildings are under consideration. The measured collector performance in all the systems matches the theoretical collector efficiency curve with a maximum deviation of five percentage points. Depending on the individual system configurations, the specific annual yield ranges between 174 kWh/m<sup>2</sup> and 445 kWh/m<sup>2</sup>. During stagnation, we report a maximum temperature between 105 °C and 127 °C. In comparison to state-of-the-art systems, the maximum temperature in the solar circuit is 80–100 K lower and evaporation does not occur. The approach leads to reductions in investment costs of up to 16% and can significantly decrease the annual maintenance effort. Assuming a system lifetime of 25 years, we estimate a cost reduction of up to 22% in Levelized Cost of Heat (LCoH) compared to common system configurations.

## 1. Introduction

Solar thermal systems are used to cover significant parts of the heat demand for the domestic hot water supply and space heating of buildings. Depending on the design of the plant and the heat demand, more or less intensive stagnation periods can occur. To handle stagnation loads usually requires a complex hydraulic system design impairing the operational safety and leading to high maintenance costs, which make solar thermal systems generally more expensive and less attractive. Thus, a significant reduction of the stagnation load can help to increase the share of solar thermal energy in an efficient and safe way. In order to prevent overheating, different approaches are pursued. Most of them are based on cooling systems or collector draining strategies (drainback), which require additional components and control technology respectively. Other technologies operate directly inside the collector, at the point where the solar irradiance is absorbed and heats up the heat transfer fluid of the solar circuit.

In flat-plate collectors (FPC), the reduction of stagnation time can be achieved by rear convection cooling, as demonstrated in Har-

ison et al. [1], and Kessentini et al. [2], as well as by thermochromic absorber coatings, (see Müller et al. [3]). Attention should also be drawn to the work of Zenhäusern et al. [4], which describes a thermomechanical device to shift the absorber towards the collector glass cover and increase the ambient heat losses. The convection cooling system uses a thermally activated valve to open a channel to the ambient air, resulting in an increased heat loss. Experimental tests on prototypes prove a reduction in the maximum temperature from 155 °C to 122 °C compared to a reference collector and almost identical behavior in the operating range. In the case of the thermochromic absorber coating, the emissivity of the coating increases from 5% to 40% when a temperature of approx. 70 °C is exceeded. With new material mixtures in the absorber layers, larger switching ranges of the emissivity can also be achieved as the current research of Ditrlich et al. [5] shows. For thermochromic absorbers already available on the market, the increase in the radiation heat losses leads to a reduction in the stagnation temperature from 195 °C to 164 °C. The absorber shift to the collector glazing can reduce the maximum temperature to about 100 °C. However, the operating behavior of the collector is still too strongly

\* Corresponding author.

E-mail address: [schiebler@isfh.de](mailto:schiebler@isfh.de) (B. Schiebler).

Abbreviations	
abs	absorber
Al	aluminum
amb	ambient
aperture	aperture area
aux	auxiliary
bal	ballast
boil	boiling
chap	chapter
col	collector
Cu	copper
DHW	domestic hot water
EPDM	ethylene propylene diene monomer rubber
ETC	evacuated tube collector
exp	expansion
fin	final energy
FPC	flat-plate collector
GFK	glass-fiber reinforced plastic
HP	heat pipe
max	maximum
PE	polyethylene
ref	reference
SCF	solar circuit fluid
sol	solar thermal
stag	stagnation
sys	system
tank	heat tank
Symbols	
$A$	area in $m^2$
$a_1$	linear heat loss coefficient without power shut-off in $W/(m^2K)$
$a_2$	quadratic heat loss coefficient without power shut-off in $W/(m^2K^2)$
$E$	solar irradiation in $kWh/m^2$
$G$	global irradiance in $W/m^2$
$LCoH$	levelized cost of heat in $€ct/kWh$
$m_{stag}$	slope of power shut-off in $W/(m^2K)$
$\dot{m}$	mass flow rate in $kg/h$
$p$	pressure in bar
$Q_{aux}$	auxiliary energy in $kWh$
$Q_{sol}$	solar thermal yield in $kWh$
$q_{sol}$	specific solar thermal yield in $kWh/m^2$
$Q_{sh}$	thermal energy for space heating in $kWh$
$q_{sh}$	specific energy for space heating in $kWh/m^2$
$sf$	solar fraction in %
$T^*$	corrected temperature difference in $K$
$U$	internal heat transfer coefficient in $W/m^2K$
$U_{int}$	internal heat transfer coefficient in $W/(m^2K)$
$U_{loss}$	heat loss coefficient in $W/(m^2K)$
$V$	volume in $m^3$
$\alpha$	inclination angle in $^\circ$ ( $0^\circ = \text{horizontal}$ )
$\gamma$	azimuth in $^\circ$ ( $0^\circ = \text{south}$ )
$\vartheta$	temperature in $^\circ C$
$\eta_0$	zero-loss coefficient

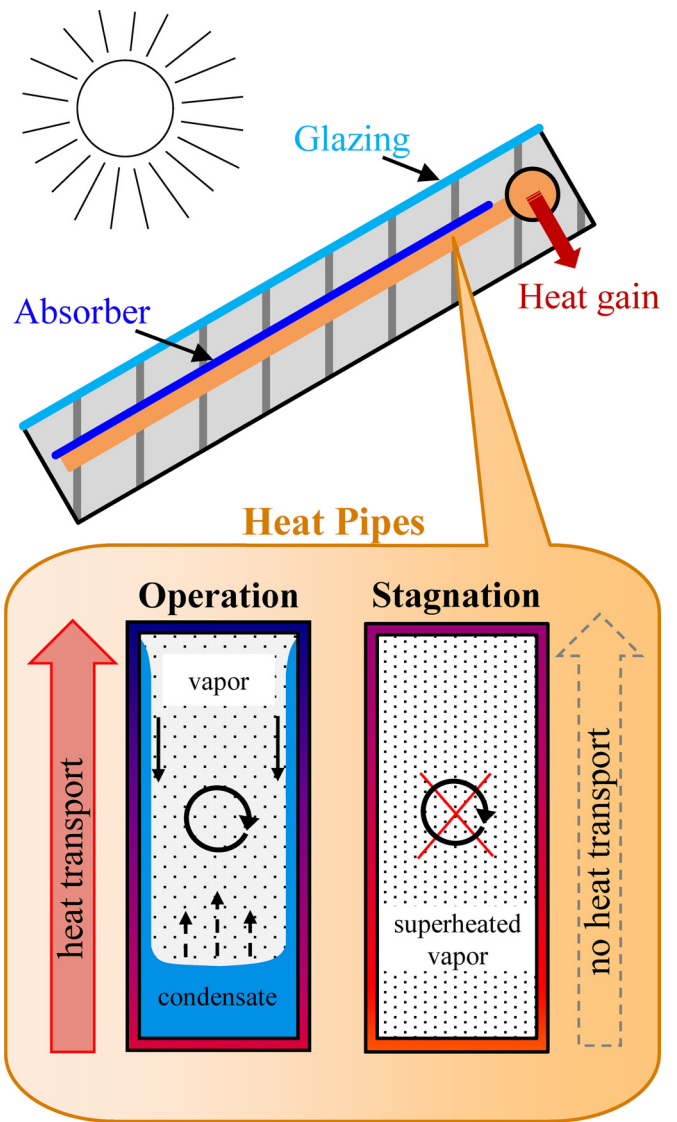


Fig. 1. Sectional view of a heat pipe collector as well as the heat pipe itself in operating and stagnation state.

affected by the switching mechanism and the concept is still under development.

For evacuated tube collectors (ETC), only solutions based on heat pipes are known to the authors. The company Kingspan used a bimetallic disk to separate the evaporator section of the heat pipe from the condenser section at a certain temperature [6]. However, the corresponding product is no longer available on the market. The approach described in this paper uses the thermo-physical properties of the heat pipe working

fluid to limit the heat transfer to the manifold section at high temperatures, as shown in Fig. 1 and demonstrated in Schiebler et al. [7]. The thermal load in stagnation states is locally limited to the absorber part of the collector, whereas the maximum temperature in the solar circuit and thus the system load can be significantly reduced. In comparison to all the other solutions, this concept enables lower maximum temperatures and is independent of mechanically loaded moving parts, i.e. is intrinsically safe. The companies Viessmann [8] and Narva [9] already use this approach, whereby in [8] the maximum temperatures are so far still above typical boiling temperatures of solar circuits. A suitable design for the temperature limitation can completely avoid evaporation of the heat transfer fluid in the solar circuit. In recent years, this approach has also been successfully integrated in FPC, as shown by Schiebler et al. [10].

The suppression of steam formation in a solar thermal system significantly increases its operational safety and enables a simpler design of the system components. Most of the literature deals with the collector development itself and the possibilities to decrease stagnation load, whereby the optimization of the solar circuit with its components is not addressed. In the context of collectors with temperature limitation and drain-back systems, a few approaches for more cost-effective system

solutions are discussed, for example by using polymeric pipes and GFK heat tanks (glass-fiber reinforced plastic). Such a promising solution is specified by Philippen et al. [11,12]. However, this concept and its feasibility were investigated only theoretically, because an intrinsically safe collector with temperature limitation has not yet been fully developed. This also seems to be the reason why the system behind the collector has not been modified up to now.

## 2. Optimized system concept

Our cost-optimized system concept consists of heat pipe-based collectors with intrinsically safe temperature limitation (see chapter 2.1). For the piping of the solar circuit, we use polymeric pipes instead of common metal pipes in a similar way as in [11], factor 3–7 downsized expansion vessels and no cooling vessels as well as an optimized solar station (see illustration in Fig. 2). This concept leads to lower investment costs and significantly reduced thermomechanical stress thanks to the prevention of overheating, which has a positive effect on the maintenance effort over the system lifetime. In the context of this research, we built five demonstration plants and equipped them with measurement technology to verify this novel cost-optimized concept (see chapter 3 and 4).

### 2.1. Collectors

The novel system concept is based on heat pipe collectors with overheating prevention, as schematically illustrated in Fig. 1 and comprehensively discussed in [7] for ETC and in [10] for FPC. The current collector prototypes were developed in cooperation with the companies AKOTEC (ETC) and KBB (FPC). With these collectors, we carried out indoor performance measurements to determine the zero-loss coefficient as well as the whole collector efficiency curve. Fig. 3 shows the FPC during the tests in our sun simulator. The results of the performance measurement of the heat pipe-based collectors are drawn with respect

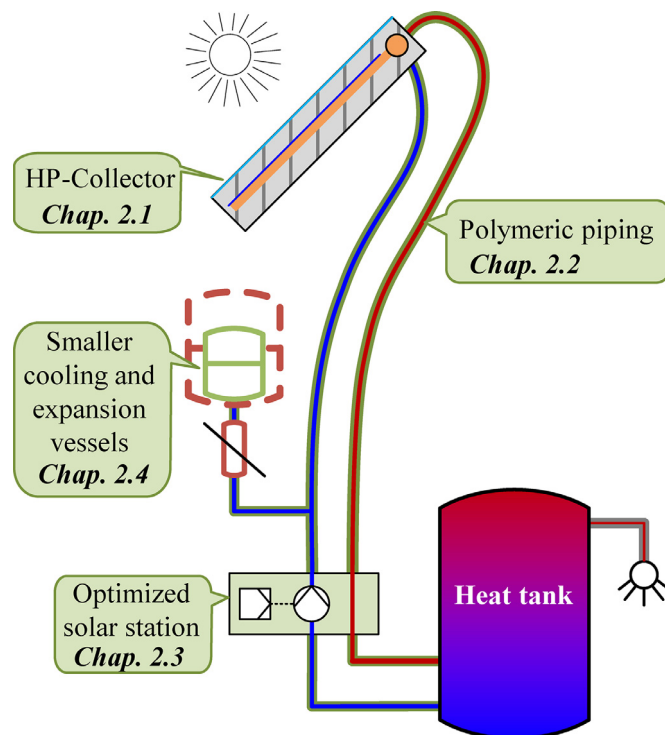


Fig. 2. Solar circuit configuration of an optimized solar system with overheating prevention.

to aperture area in Figs. 4 and 5 compared with a similar standard collector curve (direct-flow collector).

In the case of the heat pipe FPC (variant b), the zero-loss coefficient  $\eta_0$  is 0.73 (hemispherical with respect to aperture area) and thus about 0.1 points lower than for the standard direct-flow collector (variant a), as shown in Fig. 4. Both collectors feature comparable design, e.g. in each case we use glass covers with anti-reflective coatings. The difference is due to the additional thermal resistances along the heat transport path of the collector and can be expressed by the overall internal heat transfer coefficient  $U_{int}$ . Whereby  $U_{int}$  of the standard FPC (a) is about 85 W/(m<sup>2</sup>K), the FPC with heat pipes (b) reaches only 21 W/(m<sup>2</sup>K). The heat pipe-based thermal resistances for a FPC and their effect on the collector efficiency is fully described by Schiebler et al. [10]. In the operating range, the heat loss coefficient  $U_{loss}$  of both heat pipe and standard collector have approximately the same values. At temperatures above 70 °C,  $U_{int}$  of the heat pipe collector drops and  $U_{loss}$  increases significantly due to the beginning dry-out process, which can be noticed from the characteristic kink in the efficiency curve. As a result, the fluid temperature in the solar circuit of the heat pipe collector at stagnation is below 110 °C (measured without wind), which is significantly lower compared to 212 °C of the standard collector, as given in [13].

In the case of the heat pipe ETC (variant b and c), the zero-loss coefficient  $\eta_0$  is 0.72 (hemispherical with respect to aperture area) and thus about 0.05 points lower than at the standard direct-flow collector (variant (a)), as shown in Fig. 5. The difference is also due to the additional thermal resistances along the heat transport path of the collector and is in the typical range for the two different collector configurations. The overall internal heat transfer coefficient  $U_{int}$  of the considered standard ETC is about 127 W/(m<sup>2</sup>K) and that of the heat pipe ETC only 16 W/(m<sup>2</sup>K). The difference is much greater than that of the FPC, however, the effect on  $\eta_0$  is lower due to the lower heat loss coefficients  $U_{loss}$ . Similar to the FPC the heat pipe shut-off leads to a characteristic kink in the collector efficiency curve at a higher temperature level. We investigated two variants that differ only in their temperature limitation. Variant (b) shows the kink at 78 °C and variant (c) at 50 °C. We report their maximum temperatures at 128 °C (b) and 112 °C (c) under stagnation conditions (measured without wind). These temperatures are significantly lower than the given stagnation temperature of the direct-flow ETC (variant (a)) with 280 °C [14].

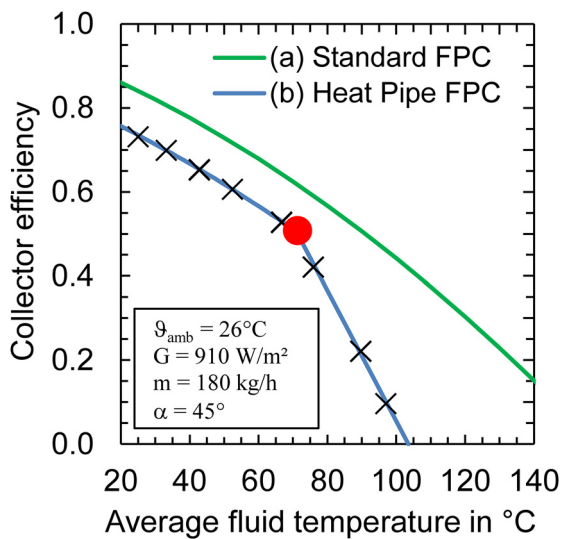
With both the FPC and ETC, the thermal output and efficiency curves can be switched in a targeted manner and the maximum temperature in the solar circuit can be significantly limited. The modeling of the heat pipe-based temperature limitation in the TRNSYS simulation program and corresponding solar yield simulations are discussed in a separate publication (see in [15]). The intrinsically safe avoidance of critical system temperatures and evaporation of the heat transfer fluid is the basis for an optimized system concept with novel system components, which is described in the following sections.

### 2.2. Solar circuit piping

The solar circuit of the innovative systems consists largely of a polymeric-based composite pipe instead of typical metal-based pipes (see Fig. 6). The multi-layer composite piping system used can be handled in a similar way to conventional copper pipes. The solutions used (pipe and connector) are exclusively standard components from the heating industry. These are usually approved for up to a maximum temperature of 95 °C, some manufacturers specify temperatures up to 110 °C for short exposure periods. In order to avoid material damage, we limit the operation of the system by properly setting the controller for temperatures below 95 °C. For indoor piping sections, pre-insulated pipes with PE foam can be used. For outdoor sections, weather-resistant EPDM insulation is strongly recommended. Since the temperatures at the collector connections and close to the collector (0.8–2.5 m) can exceed the allowed maximum temperature, we still use metallic connection pieces there, depending on the configuration. These connection pieces



**Fig. 3.** One of the FPC prototypes during laboratory tests carried out in the institute sun simulator device.

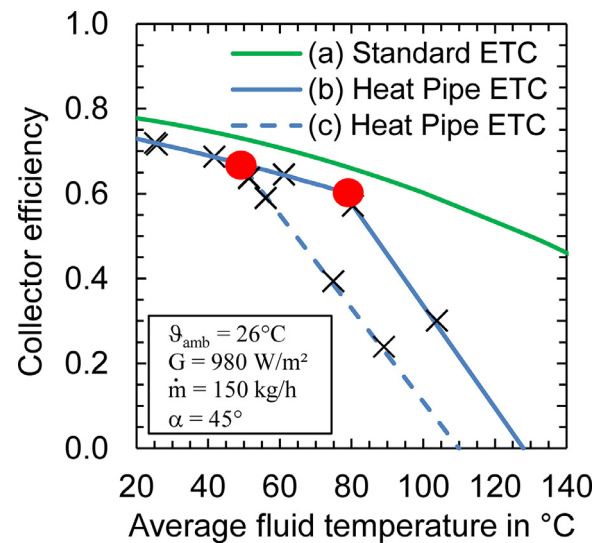


**Fig. 4.** Measured efficiency curve of the heat pipe-based FPC with respect to aperture area in comparison with a similar standard collector curve (direct-flow collector), as given in [13].

are nowadays a standard solution and are usually supplied in suitable lengths with the collectors.

### 2.3. Solar station

Due to the heat pipe-based temperature limitation, large parts of the solar circuit are exposed to significantly lower thermomechanical loads than those, which usually occur in solar thermal systems. Thus, the solar station and adjoining components are also part of our system optimization. The components of the most state-of-the-art solar stations are made of temperature-resistant materials, so that they can withstand temperatures of about 160 °C in case of stagnation [18]. Our starting point of optimization is an existing two-line solar station manufactured by the German company PAW [19]. In this case, the flow and return pipe as well as the ball valves and the pump base are integrated into a polymeric-composite block (see Fig. 7). First, we investigated this solar station experimentally in the laboratory under appropriate load conditions and then installed two pieces in the demonstration plants. Based on these experiments and taking into account the expected load tem-



**Fig. 5.** Measured efficiency curve of the heat pipe-based ETCs with respect to aperture area in comparison with a similar standard collector curve (direct-flow collector), as given in [14].

peratures, we identified possible design improvements in cooperation with the manufacturer. The corresponding cost savings potential was included in the economic evaluation (see chapter 5).

### 2.4. Pressure holding

In practice, critical states in solar thermal systems often occur due to a failure properly to consider stagnation problems. The correct dimensioning of expansion, cooling or ballast vessels is not insignificant and requires a detailed consideration of the individual system and the specific installation situation. Safety factors can compensate for planning failures, but are associated with high costs. The main uncertainty is due to the evaporation of the heat transfer fluid in the collector field during stagnation and the required expansion volume, which is related to the emptying of the collectors and the transportation of the boiling fluid into large parts of the system.

As part of our research, we examined existing design guidelines for expansion vessels and ballast vessels to determine the current state of the art. Our focus on this was in the German-speaking area. Some Ger-

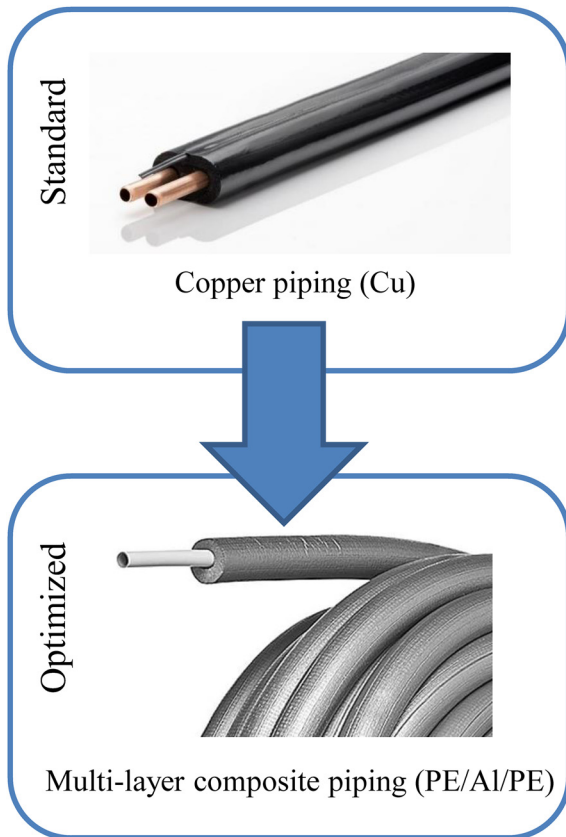


Fig. 6. Copper piping as standard component [16] and polymeric based multi-layer composite piping as optimized variant [17].

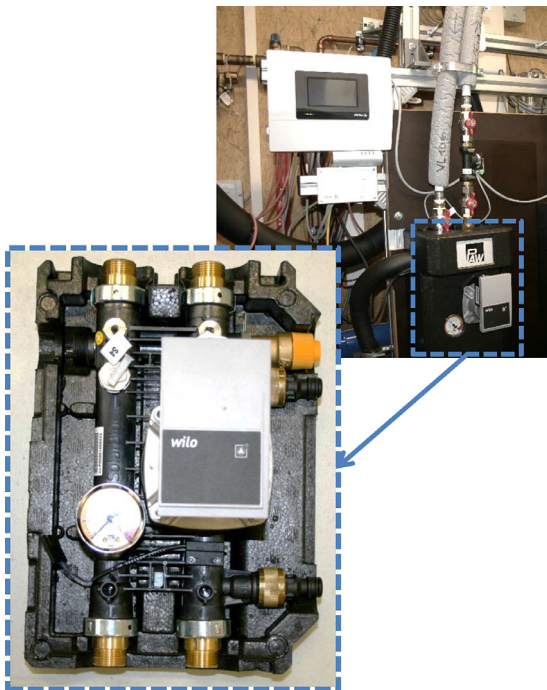


Fig. 7. Polymeric-based solar station in an optimized heat pipe system, as described [19].

man standards for example, do not address the evaporation or give only general statements for the steam volume [20–22]. This can lead to an underestimation of the steam volume, as our measurements have shown. Other rules only refer to manufacturer specifications [23]. A useful design guide from a practical point of view is provided by the planning manuals of the companies Viessmann [24] and Reflex [25], the calculation manual being used for the reference analysis in our considerations. For the use of heat pipe-based solar collectors with the avoidance of steam formation in stagnation mode, the uncertainties mentioned do not apply. The expansion vessel is only required for single-phase volume changes, so that the size of this component can be reduced by a factor of 3–7 depending on the individual plant configuration. A cooling or ballast vessel is usually installed in front of the expansion vessel to protect it from high temperatures and steam. In our expectations, the cooling vessel can be omitted with heat pipe collectors as its cooling capacity is not needed anymore (see Fig. 2). Consequently, the total volume of the hydraulic circuit is reduced, so that also significantly less solar circuit fluid (water/glycol mixture) is required.

### 3. Test- and demonstration plants

#### 3.1. Overview of the installations

Table 1 shows important system parameters of the demonstration plants, such as system type, gross collector areas  $A_{col}$  and heat tank volume  $V_{tank}$ . Furthermore, the size of the expansion vessel  $V_{exp}$  and the ballast vessel  $V_{bal}$  used are listed in relation to the reference design, which uses direct flow collectors. The amount of plastic-based piping  $L_{PE}$  is also given. The monitoring program includes two FPC and three ETC systems, whereby in two cases the collectors are used exclusively for DHW preparation and in three cases they are also used to support space heating (combi-systems). In addition to the collector, the combi-systems have two auxiliary heating systems, such as gas boilers and wood stove fireplaces.

The **DHW-system FPC 1** is part of the test plant installed at the institutes facilities and is operated in parallel with a comparable reference system with direct-flow FPC. The test procedure that we have applied for both plants corresponds to the dynamic system testing methodology (DST) according to the ISO 9459–5 [26]. The heat pipes of the FPC are designed for a maximum temperature of 110 °C. In the heat pipe system FPC 1, we only use polymeric pipes for the complete solar circuit (including the collector nearside area). The technical data of the reference collector FPC 1, such as hydraulic specifications, correspond to the manufacturers data sheet [27]. The performance parameters can be taken from the corresponding certificate [13].

The **combi-system FPC 2** assists the DHW preparation as well as the space heating system of a single-family house. The collector area corresponds to the typical dimensioning for such a solar thermal system. As in FPC 1, we use heat pipes with a maximum temperature of 110 °C.

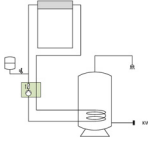

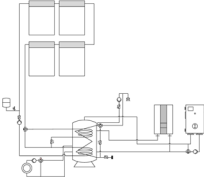

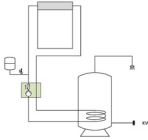

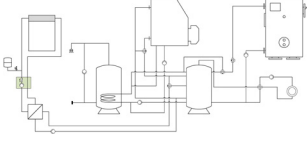

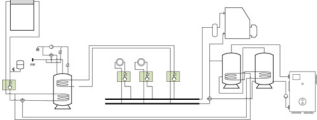

The **DHW-system ETC 1** is installed in an office building with adjacent manufacturing areas. Three collectors were mounted on the facade spaced approx. 3 m apart to take the existing window areas into consideration. The system feeds exclusively into a DHW tank and can thus cater for corresponding loads in the building's kitchen, WC and showers. The collector area of this system was intentionally oversized in order to achieve significant stagnation periods. The heat pipes of the ETC limit the maximum standstill temperature to 110 °C in the solar circuit.

The **combi-system ETC 2** is part of the central heating system of a single-family house and represents a standard system dimensioning. The collector area consists of three individual fields on the saddle roof on the front of the main building. The heat pipes of the ETC are designed for a maximum standstill temperature of 125 °C in the solar circuit.

The **combi-system ETC 3** supplies heat to a residential and seminar building as well as to a neighboring guesthouse. At this site, we replaced the existing defective FPCs with new ETCs. Therefore, we kept the existing copper solar pipe instead of installing new polymeric piping. As in

**Table 1**

Overview of the demonstration plants FPC 1–2 and ETC 1–3 with the individual collector area  $A_{col}$  (gross area) and heat tank volume  $V_{tank}$ , as well as the volume of expansion vessel  $V_{exp}$ , the volume of ballast vessel  $V_{ball}$ , the volume of solar circuit fluid  $V_{SCF}$  and the length of polymeric piping  $L_{PE}$  in comparison to a usual plant design.

Variant	Specifications	Hydraulic scheme	Collector field
FPC 1 (at institute test field)	Type: DHW $A_{col}$ : 5 m <sup>2</sup> $V_{tank}$ : 0.3 m <sup>3</sup> $V_{exp}$ : 18 l instead of 50 l $V_{ball}$ : 0 l instead of 12 l $V_{SCF}$ : 22 l instead of 33 l $L_{PE}$ : 20 m of 20 m		
FPC 2 (external)	Type: Combi $A_{col}$ : 20 m <sup>2</sup> $V_{tank}$ : 1 m <sup>3</sup> $V_{exp}$ : 20 l instead of 140 l $V_{ball}$ : 0 instead of 35 l $V_{SCF}$ : 80 l instead of 115 l $L_{PE}$ : 22 m of 27 m		
ETC 1 (external)	Type: DHW $A_{col}$ : 8 m <sup>2</sup> $V_{tank}$ : 0.3 m <sup>3</sup> $V_{exp}$ : 18 l instead of 80 l $V_{ball}$ : 0 l instead of 18 l $V_{SCF}$ : 27 l instead of 45 l $L_{PE}$ : 17 m of 22 m		
ETC 2 (external)	Type: Combi $A_{col}$ : 17 m <sup>2</sup> $V_{tank}$ : 0.15+1 m <sup>3</sup> $V_{exp}$ : 18 l instead of 80 l $V_{ball}$ : 0 l instead of 18 l $V_{SCF}$ : 27 l instead of 52 l $L_{PE}$ : 23 m of 28 m		
ETC 3 (external)	Type: Combi $A_{col}$ : 11 m <sup>2</sup> $V_{tank}$ : 1 + 2 m <sup>3</sup> $V_{exp}$ : 18 l instead of 80 l $V_{ball}$ : 0 l instead of 25 l $V_{SCF}$ : 60 l instead of 95 l $L_{PE}$ : 0 m of 50 m		

ETC 2 heat pipes are used, which limit the maximum temperature of the solar circuit to 125 °C. However, it would also be possible to use polymeric pipes with a share of about 90% in this plant. In the light of the comparatively high heat demand for DHW load, circulation and space heating, the collector field is too small, but there was no more roof area available.

### 3.2. Measurement equipment

For the energy evaluation of the plants corresponding practical requirements for the measurement technology need to be fulfilled. Due to the limited budget and the desired simple mounting, in some cases we use less expensive sensor technology. Further requirements are:

- Robustness of the sensor technology and the whole measuring systems to reduce very time-consuming troubleshooting on site
- Online access to data loggers as well as simple visualization and access to measurement data
- Hygienic requirements with regard to drinking water installations, so that the energy balance in the DHW is realized by means of pipe contact sensors and certified water meters

Based on these requirements, we developed a measuring concept that can be easily applied and adapted to the different system configurations of the plants. Fig. 8 shows a representative system configuration with the most important measuring points. In the solar circuit, the volume flow is determined with a low-cost vortex flow meter. In addition to

the reduced accuracy of the flow measurement, the temperature sensors used also exhibit deviations. Consequently, the solar yield measurement has quite high uncertainties, so we carried out additional calibration measurements to increase the accuracy. Thus, the solar yield (primary circuit) is measured with an uncertainty of about  $\pm 7\%$ . In the heating circuits of the solar combi-systems we use appropriately preconfigured and calibrated heat energy meters. In contrast to the DHW circuit, immersed sensors measure the temperature. The uncertainty of the energy recorded in the heating circuits is  $\pm 2\%$  [28]. In the DHW circuits, digital water meters are used for hygiene reasons, which work based on the ultrasonic principle. Immersed sensors for temperature measurement are not possible for hygiene reasons, so that we use pipe contact sensors (Pt1000) for the cold and hot lines. We calibrated both sensors before installation. An analysis of the uncertainties for such a determination of the DHW loads came to about  $\pm 7\%$ . Additionally, we use simple pipe contact sensors at different sites in the solar circuit, especially at the collector connections and in the area near the collector. Together with the pressure measurement at the expansion vessel, this equipment allows a proper evaluation of stagnation events. In the solar thermal plants in the institute test field both the expansion vessel of the innovative plant and that of the reference plant were calibrated in accordance with Scheuren [29], which is necessary to determine steam volume and steam expansion.

At the collector level, we measure ambient temperature and humidity as well as global irradiance by means of pyranometers. In the FPC 1 plant in the institute test field, the measurement concept described

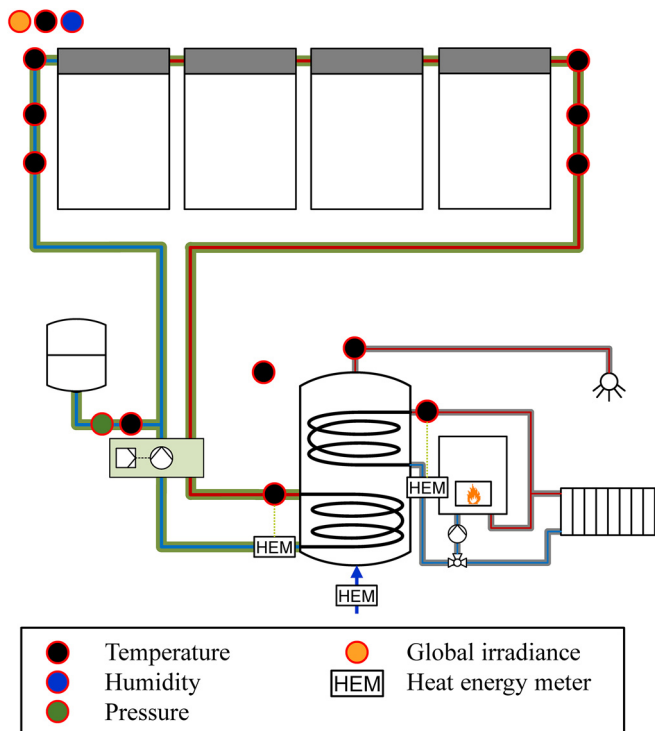


Fig. 8. Schematic illustration of the measurement concept for recording the energy flows in solar, domestic hot water and any heating circuits, as well as the temperature along the solar circuit piping, system pressure and ambient conditions (temperature, solar irradiance and humidity).

was operated in parallel to a laboratory measurement system with high-quality sensors and data acquisition within the framework of the DST tests. The comparison shows, that the simplified measurement technique does not significantly influence the result within the DST procedure. The solar yields recorded differ by only about 2% compared to the laboratory measurement technique.

#### 4. Experimental investigations

The aim of the monitoring is the practical evaluation of the heat pipe collectors and the testing of the temperature limitation in different system configurations. Based on representative measurement periods, we evaluate the behavior in operation, system yields and the practicability of the innovative system concept.

##### 4.1. Collector output

The collector and the shut-off characteristics are sufficiently known for both the ETC and FPC used from the performance measurements on the single modules (see Figs. 3 and 4). Based on the measured collector power, the reference to the efficiency characteristic is obtained for all test systems. In Figs. 9 and 10, the measured collector efficiencies in the plants are plotted in comparison to the curves of the single module over the temperature difference  $T^*$ , whereby the collector output was experimentally determined by means of a vortex flow rate sensor and temperature pipe contact sensors. The focus of the illustrations in Figs. 9 and 10 is more on the functional control rather than on the quantitative evaluation of the collector efficiency. Corrections due to the incident angle and direct/diffuse solar radiation contributions are not considered, but have a small impact on the results. Based on the selected measurement points (about 10 min steady state), we can verify the performance of the heat pipe collectors in the field application. For all plants, the deviation of the real collector efficiencies from the theory is at most 5 percent-

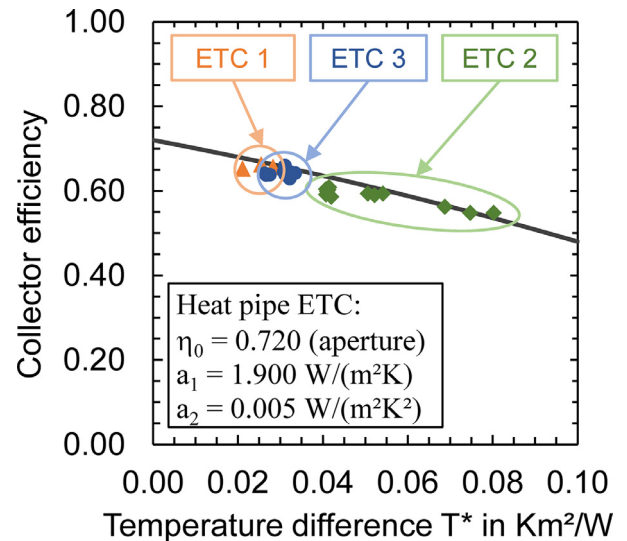


Fig. 9. Measured collector efficiencies of the ETC systems over the temperature difference  $T^* = (\vartheta_{\text{fluid}} - \vartheta_{\text{amb}}) / G$  in comparison to the measured efficiency curve of single modules.

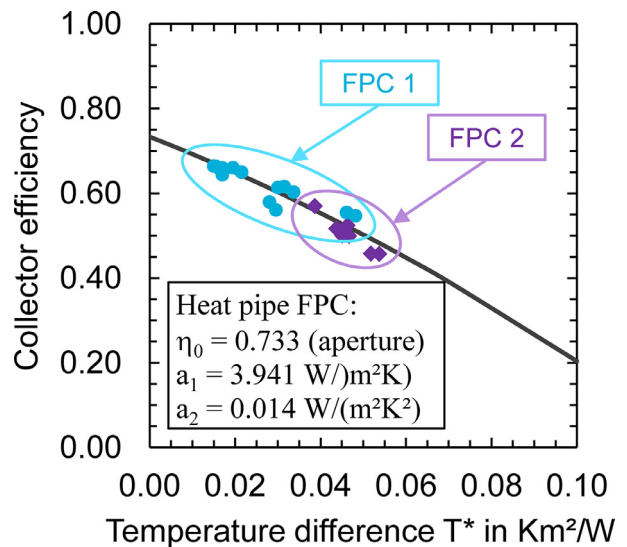


Fig. 10. Measured collector efficiencies of the FPC systems over the temperature difference  $T^* = (\vartheta_{\text{fluid}} - \vartheta_{\text{amb}}) / G$  in comparison to the measured efficiency curve of single modules.

age points, which is a good approximation taking the simplicity of the comparison into account.

In addition to the behavior within the operating range of the heat pipes, we also consider the collector performance in the shut-off range. Figs. 11 and 12 show the results for two ETC systems and two FPC systems over the average fluid temperature. The efficiency approximates well in each case the described shut-off function. The behavior of the heat pipe collectors in the demonstration plants thus corresponds to the expected curve over the whole temperature range.

##### 4.2. Stagnation load

For all systems, stagnation events were investigated in the summer of 2020 and 2021 in order to evaluate the thermal load at critical points, e.g. at the collector connections and along the PE/Al/PE-composite pipe. For this purpose, the collectors are divided into two categories or shut-off temperatures of approx. 110 °C and approx. 125 °C (in dependency of heat pipe design).

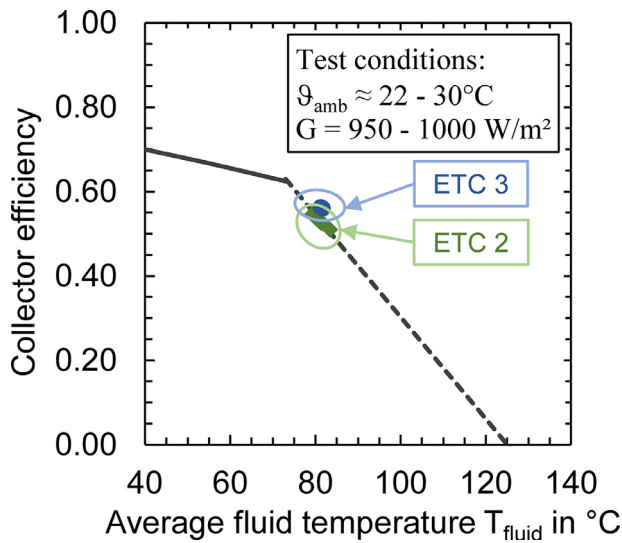


Fig. 11. Measured collector efficiencies in the heat pipe power limitation range of ETC 2 and ETC 3 in comparison to the theoretical characteristic curve and the predicted shut-off curve.

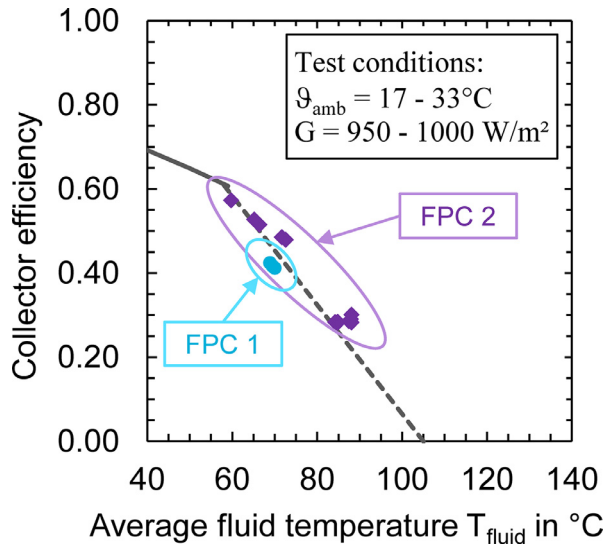


Fig. 12. Measured collector efficiencies in the heat pipe power limitation range of FPC 1 and FPC 2 in comparison to the theoretical characteristic curve and the predicted shut-off curve.

Fig. 13 shows the temperature curves of a stagnation event in the DHW-system FPC 1 (test plant at the Institute), with a common operating pressure  $p_{sys} > 1 \text{ bar}$ . This case can be classified as a typical stagnation event. The maximum temperature of  $105^\circ\text{C}$  is measured at the collector (solar circuit), far below the boiling point of  $126^\circ\text{C}$ . The nearly pressure-less condition ( $p_{sys} \approx 0.4 \text{ bar}$ ), shown in Fig. 14, is intended to represent a so-called "worst-case" scenario, where the pressure drop can result e.g. from a creeping leak. For these tests, in contrast to the innovative system concept, a large expansion vessel volume is used in order to compensate the pressure increase due to steam formation and to keep the collector temperature above the boiling point for as long as possible. The results for this extreme case show that the temperature at the collector or manifold reaches  $107^\circ\text{C}$  and thus the boiling point, although only small amounts of steam volume are generated.

In addition to the maximum temperature and individual boiling point at collector level, Fig. 15 also shows the steam volume produced during stagnation events for all demonstration plants. In general, the

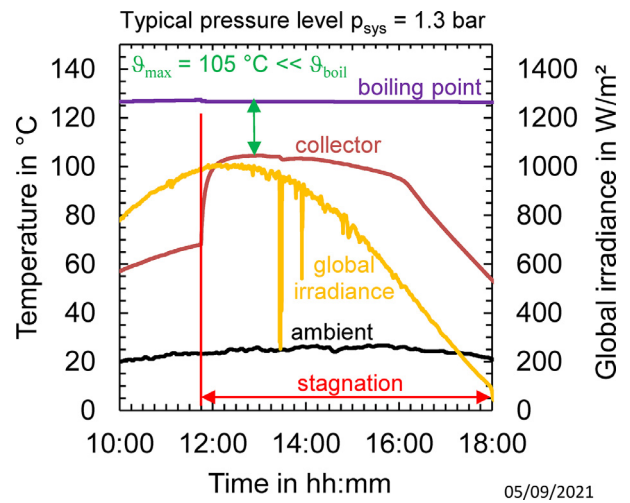


Fig. 13. Temperature over time of a stagnation day of FPC 1 at typical operating pressure ( $p_{sys} = 1.3 \text{ bar}$ ).

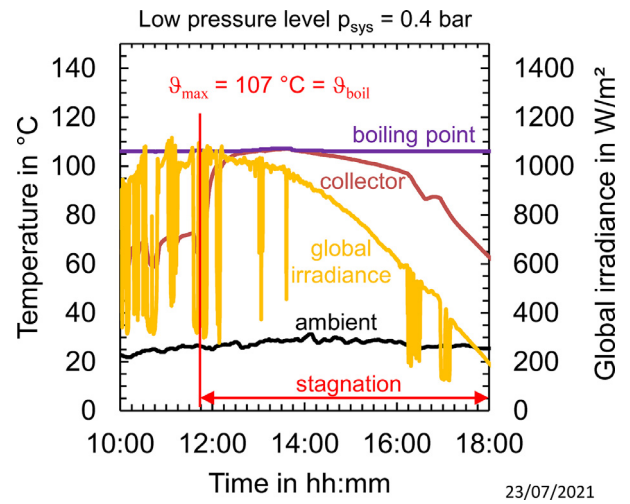


Fig. 14. Temperature over time of a stagnation day of FPC 1 at low operating pressure ( $p_{sys} = 0.4 \text{ bar}$ ).

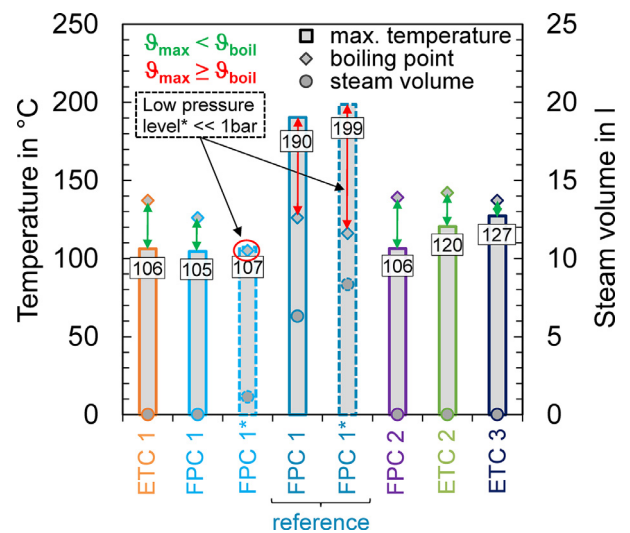


Fig. 15. Maximum temperature and boiling point as well as steam volume as a result of the stagnation events in the demonstration plants; for FPC 1 with typical system pressure and reduced system pressure\* ( $\ll 1 \text{ bar}$ ) as well as in comparison to the reference system with direct-flow FPC.



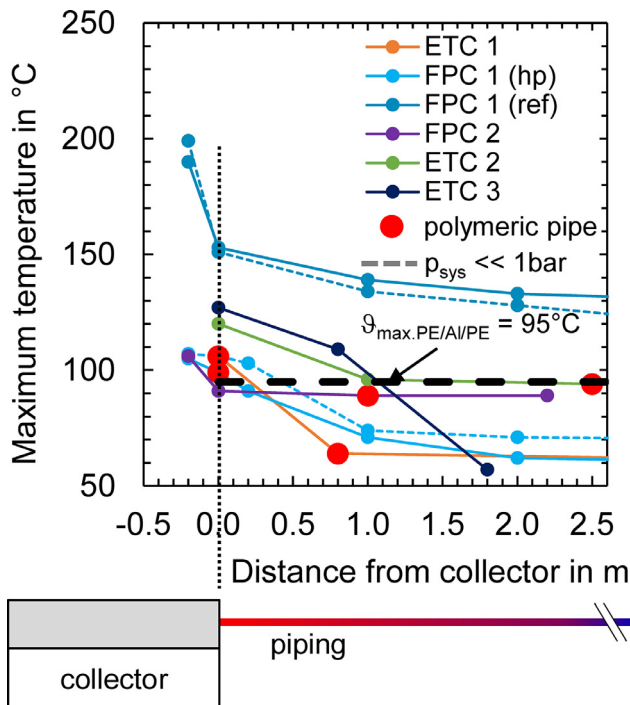


Fig. 16. Maximum temperature at stagnation along the pipe in the close range of the collector (0 m = collector connection) for all systems considered (red = connection to the polymeric pipe).

maximum temperature in the solar circuits with heat pipe collectors is between 105 °C and 127 °C, depending on the collector configuration. For a typical system pressure level ( $p_{sys} > 2$  bar), the boiling point at the collector is not reached in any of the systems, so that critical evaporation processes can be avoided. The considered reference system (FPC 1 reference) has identical system dimensions as the DHW-system FPC 1 with heat pipes and is always operated in parallel. In the reference system, significantly higher temperatures of about 190 °C and 199 °C respectively are recorded in the solar circuit and the steam volume lies between 6 l and 8 l (depending on pressure level) because the boiling point is exceeded. For the extreme case ("worst case") with very low pressure, the heat pipe system of FPC 1 also reaches the boiling point, whereby the amount of steam is only about 1 l and thus limited to the collector or manifold section. A relevant expansion of the collector's temperature level to the piping system and other components is nevertheless avoided.

Fig. 16 shows the maximum temperature at stagnation along the pipe in the close proximity to the collector. As shown in all the demonstration plants (only heat pipe) the maximum temperature of 95 °C, which is relevant for the use of polymeric piping, is no longer significantly exceeded from approx. 1 m and reliably undercut from 2.5 m onwards. In the case of heat pipe system FPC 1, the maximum temperature at the collector connections is below 100 °C and even at a distance of 0.2 m from the collector, temperatures above 95 °C no longer occurred. For the "worst case" with evaporation ( $p_{sys} \ll 1$  bar), slightly higher temperatures at the collector as well as in the close proximity (0.2 m) are recorded, because the expansion displaces the heat transfer fluid from the collector due to boiling. In this case, we measured 103 °C instead of 99 °C at position 0.2 m.

The red dots in Fig. 16 mark the transition from the metallic collector connection pipe to the polymeric piping system, which takes place at 0 m (FPC 1 heat pipe), approx. 1 m (ETC 1, FPC 2) or 2.5 m (ETC 2), depending on the chosen design. In ETC 3 we still use the standard copper pipe for various reasons, although polymeric pipes could also be installed here from approx. 2 m onwards. Compared to all the heat pipe

systems with overheating prevention, the reference system FPC 1 shows, as expected, significantly higher temperatures in the close range of the collectors. The maximum temperature at the collector connections is approx. 150 °C and at a distance of 1 m still approx. 140 °C. In this case, the boiling process forces liquid or even vaporized heat transfer fluid at high temperatures a long way into the piping system.

The significantly smaller expansion volumes and the elimination of the cooling vessels in the heat pipe systems have no impact on the operational safety. Compared to state-of-the-art collectors (reference), heat pipe-based overheating prevention reduces the maximum solar circuit temperature by 80 - 100 K and prevents the spread of critical steam volume with an intrinsically safe approach.

### 4.3. System performance

The evaluation of system performance is based on the solar yield in the solar circuit  $Q_{sol}$ , which was measured directly in all demonstration plants in accordance with the procedure described in chapter 3.2. The average specific yield for Germany is about 378 W/m<sup>2</sup> per year for solar thermal combi-systems of single-family and multi-family houses, as given by Weiss et al. [30]. It should be noted that this performance parameter is heavily dependent on the system design (collector size and orientation, heat demand) and, that some of the plants studied do not represent typically dimensioned systems. In the case of the DHW-system FPC 1 (both heat pipe and reference) we considered the results from dynamic system tests (DST) in accordance with the ISO 9459-5 [26]. The standardized DST-method is not appropriate for collectors with such low shut-off temperatures. In our experience – also confirmed by TRNSYS simulations – this leads to a slight underestimation of the solar yield.

In addition to the solar yield, we also use the solar fraction  $sf$  as performance indicator for the systems.  $sf$  indicates what proportion of the energy demand can be covered by the solar system and directly depends on the solar yield  $Q_{sol}$  and the conventional auxiliary energy  $Q_{aux}$  (see Eq. (1)). In solar thermal DHW-systems, the proportion of  $sf$  is usually between 30 and 60%. The proportion of  $sf$  is also dependent on the system design (collector size and orientation, heat demand). For example, in Bachmann et al. [31] a typically designed DHW-system for single-family houses in Germany with a solar fraction of 40% is described. In combi-systems with space heating support, 10 to 50% is usually achievable. For example, Bachmann et al. [32] and Helbig et al. [33] specified  $sf$  for the reference systems in Germany between 20% and 31%.

$$sf = \frac{Q_{sol}}{Q_{sol} + Q_{aux}} \quad (1)$$

Table 2 shows the system specifications, such as collector area or orientation, and results after one year of operation for all demonstration plants. In addition to solar yield  $Q_{sol}$  and solar fraction  $sf$ , the energy demands for domestic hot water preparation  $Q_{DHW}$  and space heating  $Q_{sh}$  as well as the conventional auxiliary energy  $Q_{aux}$  are also given. In Fig. 17, the specific solar yield with regard to the aperture area of the collectors as well as the values of  $sf$  are shown graphically.

The specific annual yield of the demonstration plants considered ranges between 174 kWh/m<sup>2</sup> and 445 kWh/m<sup>2</sup>, whereby the solar fraction is between 5% and 93%. In the DHW-system ETC 1, we measure the lowest specific solar yield due to the intentional oversizing of the collector area. As consequence of this,  $sf$  is unusually high (> 90%). In contrast, the combi-system ETC 3 achieves the highest specific solar yield, which can be attributed to the high heat demand. In the case of the DHW-systems FPC 1 (heat pipe and reference), the solar yield is determined based on DST-measurement in parallel operation. Therefore,  $Q_{sol}$  and  $sf$  are both affected by the thermal losses in the heat tank (in accordance with the DST-assumptions). Thus, the results are more realistic, but in comparison to the performance parameters of all the other demonstration plants slightly lower. The solar yield of the systems FPC 1 rather represents a usable yield or avoided auxiliary energy. The comparison between the FPC 1 systems shows that the specific solar yield of

**Table 2**

Important parameters and results of the demonstration plants from one year of operation, for the FPC 1 (heat pipe and reference) DST results for the Würzburg site are given.

Parameter	Unit	ETC 1 (hp)	FPC 1 (hp)	FPC 1 (ref)	FPC 2 (hp)	ETC 2 (hp)	ETC 3 (hp)
$A_{aperture}$	m <sup>2</sup>	5.0	4.2	4.6	16.8	10.0	7.0
$\alpha$	°	80	45	45	45	55	25
$\gamma$	°	46	0	0	-11	5	12
$E_{sol}$	kWh/m <sup>2</sup>	919	1 267 <sup>1</sup>	1 267 <sup>1</sup>	1 176	1 045	1 200
$Q_{sol}$	kWh	868	876	1 057	5 258	4 451	3 366
$q_{sol}$	kWh/m <sup>2</sup>	174	209	230	313	445	481
$sf$	%	93	42	51	44	25	6
$Q_{DHW}$	kWh	337	2 085 <sup>2</sup>	2 085 <sup>2</sup>	2 605	1 027	6 058
$Q_{sh}$	kWh	-	-	-	5 788	12 425	51 398
$q_{sh}$	kWh/m <sup>2</sup>	-	-	-	48	104	91
$Q_{aux}$	kWh	62	1209	1 028	7 658	13 338 <sup>3</sup>	55 599

<sup>1</sup>  $E_{sol}$  of Würzburg, as DST reference location of Germany according to ISO 9459-5 [26].

<sup>2</sup> For daily tapping volume of 140 l/d.

<sup>3</sup> Estimated on the basis of pellet consumption in the 2020/2021 heating season.

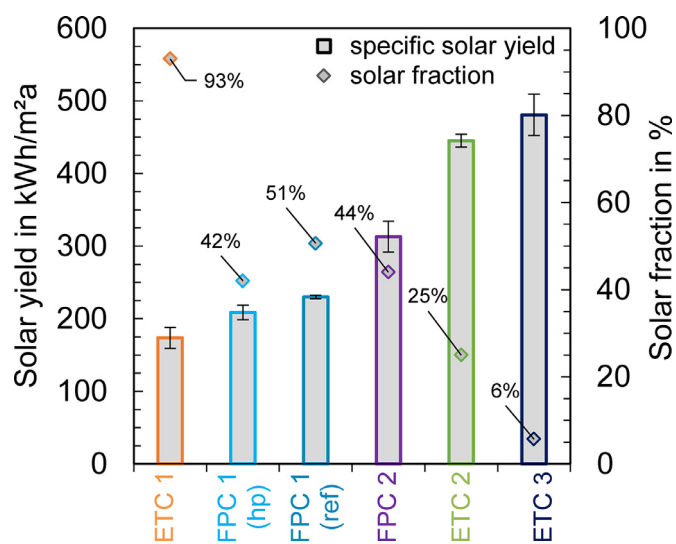


Fig. 17. Results of the specific solar yield as well as the solar fraction for the demonstration plants after one year of monitoring; the results at FPC 1 (hp) and FPC 1 (ref) are based on DST-sequences.

the heat pipe collector is 9% lower than the result of the reference system due to the additional heat resistance. The proportion of  $sf$  is 42% for the heat pipe FPC 1 and thus about nine-percentage points lower than the  $sf$  of the reference FPC 1. The three combi-systems FPC 2, ETC 2 and ETC 3 achieve almost typical solar yields. The proportion of  $sf$  is also in a common range with 44% for FPC 2 and 25% for ETC 3. Only in ETC 3 the collector field is comparatively undersized – with regard to the high heat demands (approx. 56 MWh/a for space heating and approx. 6 MWh/a for DHW) – so that the solar fraction here is only 6%.

Overall, the system performance of the heat pipe collectors with overheating prevention is demonstrated for both the ETC systems and the FPC systems. All the systems have also been modeled and studied with the TRNSYS simulation tool in parallel to the experimental evaluations. The solar yields were evaluated for each case in comparison to a reference system with direct flow collector without overheating prevention. The results of the simulation study are presented and comprehensively discussed in [15].

## 5. Cost reductions

For a holistic evaluation of the innovative system concept, we consider both the cost benefits due to overheating prevention and the individual solar yields to carry out a LCoH analysis. For this purpose, we

consider the solar circuit components of the implemented demonstration plants (see chapter 3) and the state-of-the-art components of a reference system for each case. Table 3 gives an overview of the assumptions and possible cost advantages of the components. For example, the polymeric-based pipe system leads to a cost reduction of about 40%. Due to the mixed installation with metal pipe segments, the actual saving potentials are up to 8 percentage points lower, depending on the system configuration. For the Swiss market, Philippen et al. [11] determined the savings potential with polymeric pipes in a similar context to be 52%, which confirms our assumptions.

In addition to the component costs, we also take the installation and the maintenance costs over a period of 25 years into account. For the evaluation of the so-called "Levelized Cost of Solar Heat" ( $LCoH_{sol,fin}$ ) in accordance with the IEA TASK54, the costs of the conventional energy (i.e. final energy) are compared, which can be saved with the solar thermal system, as specified by Louvet et al. [34]. In order also to obtain these results for the reference plants with direct flow collectors, we do simulations with TRNSYS (see [15]). For the cost analysis, we use an actual test reference year with representative climatic conditions of the German reference location Würzburg, as specified by Remund and Müller [35]. We do not take the measured meteorological data in order not to affect the validity of the results through individual climate influences of the measurement periods 2020–2021. For the ETC 1 system, we use a daily DHW tapping volume of 100 l/d instead of the measured 21 l/d, which corresponds to a typical expected value. The uncommon measured value is due to the Covid19 pandemic-related reduced occupancy and correspondent demand in office and manufacturing areas.

For the installation costs, we use the data from the IEA TASK54 as a basis in accordance with the available system configurations, whereby we scale the costs depending on the individual collector areas of the demonstration plants. The underlying costs for installation come from Bachmann et al. [31] for DHW-systems, from Bachmann et al. [32] for combi-systems in single-family houses and from Helbig et al. [33] for combi-systems in multi-family houses. There are corresponding advantages for the innovative system concept, which result from the lower assembly costs for the plastic pipe installation as well as the possible synergies in material procurement and logistics, if components from the heating industry can be used for the most part in the solar circuit. For example, no special seals are required. Finally, the simpler filling and flushing of the systems with heat pipe collectors also leads to advantages during commissioning. It is difficult to quantify these points in the context of cost analysis, even with the involvement of technical partners. Accordingly, we use assumptions from a previous R&D project, as specified in [36] as a basis for the evaluation of installation costs. These assumptions were comprehensively discussed in the scope of the IEA TASK54 expert groups and described in [37].

**Table 3**  
Overview of the main assumptions taken in the evaluation of the component costs for the reference and heat pipe systems.

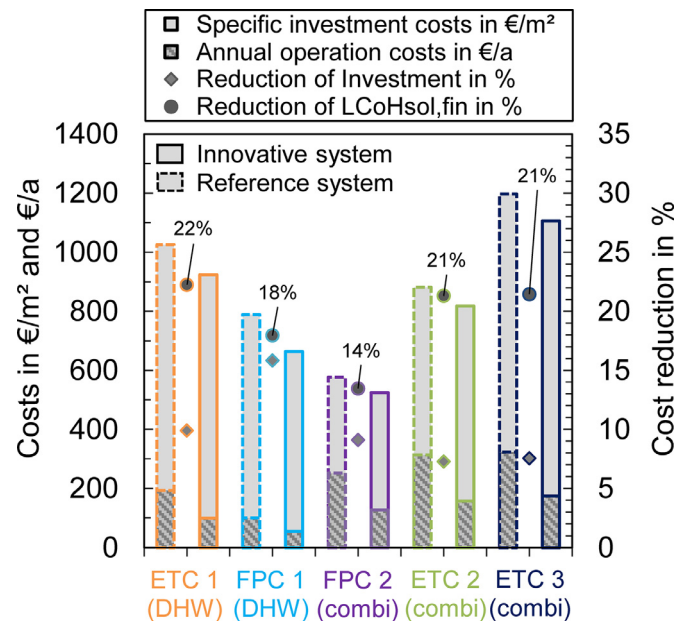
Components	Reference system	Heat pipe system	Difference in%
Collector	ETC: offer prices	ETC: offer prices	-2%
	FPC: as Bachmann et al. [31]	FPC: as Bachmann et al. [31] <sup>1</sup>	0%
Piping	Costs for metallic piping	Costs for polymeric-based composite pipe	-40%
Expansion vessel	Offer prices according to typical dimensioning	Offer prices for 3–7 times smaller expansion vessels	-70–85%
Ballast vessel	Offer prices according to typical dimensioning	Without ballast vessel	-100%
Solar station	Offer price for a standard two-line solar station	Price calculation for an optimized polymer station	-16%
Heat Tank	Offer prices for DHW-, buffer and combined heat tanks, Considerations of the <i>credit conventional heat store</i> , for the double-use in both the solar thermal system and the auxiliary system as specified in Bachmann et al. [31,32], Helbig et al. [33]	-	-

<sup>1</sup> The manifold of the heat pipe FPC will lead to additional costs even in serial production. However, costs can be saved by using aluminum heat pipes compared to copper piping in direct-flow FPCs. Therefore, we assume that both effects compensate each other and the same collector costs are possible.

The annual operating costs include the energy demand for pump and controller as well as the maintenance and servicing costs. These are determined for all plant types, as in Bachmann et al. [31], Bachmann et al. [32] and Helbig et al. [33]. In the reference case, 2% of the investment costs are assumed for maintenance and servicing. For the innovative system concept, there are advantages resulting from the lower thermo-mechanical load on the solar circuit components. This aspect plays an important role in particular for the solar circuit fluid (water/glycol mixture). Furthermore, operational breakdowns due to stagnation can also be avoided. Therefore, the hydraulics of the closed solar circuit must be opened and the system pressure released, a condition that causes system standstill, workload and additional material (all associated with corresponding costs). Similar to installation costs, such cost items are difficult to evaluate. In [36] the possible cost benefits particularly due to the longer lifetime of the heat transfer fluid were investigated. The results were evaluated and comprehensively discussed in the context of the IEA TASK54. According to this previous study the annual maintenance costs of heat pipe systems with overheating prevention is halved and can be set at 1% of the investment costs [38]. This figure is also assumed for the present cost analysis.

The  $LCoH_{sol,fin}$  for the reference systems considered (direct flow collectors and standard solar circuit components) are between 18 €/ct/kWh and 24 €/ct/kWh, based in each case on the individually determined costs and measured heat demand.<sup>1</sup> For the DHW-system ETC 1, the  $LCoH_{sol,fin}$  are extremely high (>50 €/ct/kWh) and not representative due to the oversized collector field. Fig. 18 shows the specific investment costs and annual operating costs of the innovative systems, each in comparison to the reference system. In addition, the relative savings in investment and  $LCoH_{sol,fin}$  are plotted for each site. The results of the innovative systems show that between 7% and 16% of the investment costs can be saved compared to a standard installation. The optimized pressure holding (expansion vessel and ballast vessel) represents the greatest share of these savings, with proportions between 40% and 63%. The share of investment cost reduction for polymeric pipes is 8% to 17%, depending on the system configuration. The share for a polymeric-based solar station is 5% to 9%.

The  $LCoH_{sol,fin}$  can be determined by taking the operating and maintenance costs as well as the individual usable solar yields into account. We calculate that for all the innovative demonstration plants over a pe-



**Fig. 18.** Specific investment costs and annual operating costs of the innovative systems compared to the corresponding reference system as well as illustration of the relative savings in investment and  $LCoH_{sol,fin}$ .

riod of 25 years in comparison to their individual reference systems. For ETC systems, the  $LCoH_{sol,fin}$  can be reduced by 21% and 22%, respectively, as a result of the innovative approach with heat pipe overheating prevention. In the case of the FPC systems, the solar yields are considerably lower compared to the reference collector due to the significantly lower aperture area (-9%), so that the  $LCoH_{sol,fin}$  benefits are only 14% for the FPC 2 (combi-system) and 18% for the FPC 1 (DHW-system). With respect to the  $LCoH_{sol,fin}$  savings, the cost benefits for the components (investment) play a comparatively minor role. For the optimized pressure holding, the share is still between 9% and 25%, for the polymeric piping, it is approx. 2% to 5% and for the polymeric solar station, the maximum benefit is only 1.4%. Considering the whole evaluation period of 25 a, the influence of the running costs dominates. In particular, the share of maintenance costs has the most significant effect on the  $LCoH_{sol,fin}$ .

<sup>1</sup> For the DHW-system FPC 1, a daily tapping volume of 140 l/d is used as a typical case in each case.

## 6. Conclusion

Based on solar thermal collectors with overheating prevention, we have developed a novel system concept that offers more flexibility compared to the commonly used components and design guidelines. For example, the pressure holding has significantly less requirements and the use of commercially available polymeric pipes from the heating industry is possible. We have implemented this innovative concept in five demonstration plants and evaluated their operation in a practical way based on a corresponding plant monitoring. The experimental results show, that evaporation of the heat transfer fluid and critical system conditions can be completely avoided in all the systems. Depending on the collector and system configuration, we measured the maximum temperatures as between 105 °C and 127 °C. Temperatures of 95 °C were not exceeded in the pipe at a distance of 1 m from the collector. Compared to collectors without temperature limitation, the maximum solar circuit temperature was reduced by 80 - 100 K. Within the scope of one-year operation, both the collector performance and the system yield are confirmed based on corresponding key figures.

The use of significantly smaller expansion vessels as well as polymeric pipes has proven to be unproblematic in all the plants. Nevertheless, the collector connection should be carried out with metallic pieces in the close proximity to the collector. Depending on the individual system configuration, the metal connection pieces should have a length of between 0.8 m and 2 m and can be delivered together with the collector, in accordance with a procedure which is already standard for some manufacturers today. The transition to polymeric pipes can take place after roof penetration and the pipe can easily be assembled by the installer. Due to the temperature limitation, the rest of the solar circuit can be built similarly to a normal heating circuit. This mainly concerns the thermal durability of components, including sealing materials. Furthermore, this new approach significantly reduces the risk of incorrectly designed cooling and pressure vessels and the associated consequences.

Based on a cost analysis for the components used and the assumptions for the installation procedure, the novel system concept can reduce the investment costs by 7% to 16% compared to a state-of-the-art reference system. In addition to the initial costs, we also considered the operation and maintenance costs over a period of 25 years. Taking the significantly lower thermomechanical load and a lower failure rate into account, we estimate the maintenance requirements in accordance with the previous studies on this topic. The total costs in relation to the saved conventional auxiliary energy thus result in a lower heat price ( $LCoH_{sol,fin}$ ) for the innovative system concept with heat pipe collectors in comparison to the reference. For the ETC plants considered, this cost advantage is between 21% and 22%. For the FPC plants, the differences are lower due to the unfavorable ratio between aperture and gross area as well as the associated lower solar yield. Here the benefits are between 14% and 18%. While the ETC with overheating prevention are almost ready for series production and, for specific maximum temperatures, already available on the market, the FPC are still at the prototype status. Due to the heat pipe manifold, which is not typical for FPC, and the necessary area requirements for the current technical solution, the advantage in the heat price ( $LCoH_{sol,fin}$ ) is lower for the demonstration systems considered compared to typical direct-flow FPC-systems. At this point, further work is needed to develop a more efficient and competitive FPC concept with shut-off heat pipes.

With regard to the developed system concept, all the stakeholders as system suppliers, installers and end users (operators) must decide to what extent they can and want to implement this approach. For example, manufacturers of the polymeric pipes have not approved their products for use in solar thermal systems. The considered optimized solar station is also not available on the market in this form. The cost analysis carried out as part of this study has shown that the direct cost savings of using polymeric pipes and solar station have no significant influence on the  $LCoH_{sol,fin}$ . An optimized pressure holding, on the other hand, has a strong impact on this. All the results presented are based on

corresponding assumptions, e.g. for installation and maintenance costs, which still have to be confirmed after long-term system operation. However, it is currently undisputed that the intrinsically safe prevention of critical overheating conditions and evaporation of the heat transfer fluid can offer a relevant advantage for the reliable operation of solar thermal systems and can lead to cost savings. Both aspects are crucial for the future of this technology.

## Declaration of Competing Interest

The authors declare that they have no known competing financial interests or personal relationships that could have appeared to influence the work reported in this paper.

## Acknowledgments

The project "Development and demonstration of innovative, stagnation safe solar thermal systems with heat-pipe collectors" (reference number 03ETW005A-C) underlying this publication is based, was funded by the state of Lower Saxony and the German Federal Ministry of Economy and Climate Action, following a decision of the German Parliament. The investigations were carried out in cooperation with the companies KBB Kollektorbau GmbH and AKOTEC Produktionsgesellschaft mbH.

The authors are grateful for this support. The responsibility for the content of this publication lies with the authors.

## References

- [1] S.J. Harrison, Q. Lin, L.C.S. Mesquita, Integral stagnation temperature control for solar Collectors, in: *Conference Proceedings SESCOI 2004, University of Waterloo, 2004.*
- [2] H. Kessentini, R. Capdevila, J. Castro Gronzalez, A. Oliva, Numerical simulation of heat transfer and fluid flow in a flat plate solar collector with TIM and ventilation channel, in: *Croatian Solar Energy Association, Eurosun 2012 – Conference Proceedings. Rijeka, 2012.*
- [3] S. Müller, F. Giovannetti, R. Reineke-Koch, O. Kastner, B. Hafner, Simulation study on the efficiency of thermochromic absorber coatings for solar thermal flat-plate collectors, *Sol. Energy v. 188 (2019) 865–874*, doi:10.1016/j.solener.2019.06.064.
- [4] D. Zenhäusern, S. Brunold, M.S. Maricar, M. Dudita, M. Haller, D. Philippen, Technische Ansätze zur Realisierung überhitzungssicherer Flachkollektoren – Review und eigene Entwicklungen Konferenzbeitrag, 30. Symposium Solarthermie und Innovative Wärmesysteme, in: *Conference Proceedings, Bad Staffelstein, 12.-14. Mai 2020, 2020.*
- [5] A. Dittrich, F. Heinemeyer, Ch. Xu, R. Reineke-Koch, Realization of a cost-effective thermochromic solar absorber with a high emittance change based on VO<sub>2</sub> and an infrared transparent intermediate layer, *AIP Adv. 12 (2022) 035118* 2022, doi:10.1063/5.0063702.
- [6] Kingspan, 2017. Environmental Product Portfolio – The Kingspan Guide to Our Environmental Solutions in the Middle East, Africa, Turkey, Central Asia and India. [https://ks-kentico-prod-cdn-endpoint.azureedge.net/netxstoreviews/assetOriginal/74419\\_Environmental\\_Brochure%202017\\_Brochure\\_EN\\_TR.pdf](https://ks-kentico-prod-cdn-endpoint.azureedge.net/netxstoreviews/assetOriginal/74419_Environmental_Brochure%202017_Brochure_EN_TR.pdf) (accessed 22/06/2022).
- [7] B. Schiebler, S. Jack, H. Dieckmann, F. Giovannetti, Experimental and theoretical investigations on temperature limitation in solar thermal collectors with heat pipes: effect of superheating on the maximum temperature, *Sol. Energy 171 (2018) 271–278*, doi:10.1016/j.solener.2018.06.036.
- [8] Viessmann Werke GmbH & Co. KG, 2019. VITOSOL 300-TM Vakuum-Röhrenkollektor nach dem Heatpipe-Prinzip zur Nutzung der Sonnenenergie. [https://www.viessmann.de/content/dam/public-brands/master/products/solar/vitosol-300-tm/DB-5793172\\_Vitosol\\_300-TM.pdf/\\_jcr\\_content/renditions/original.media\\_file.download\\_attachment.file/DB-5793172\\_Vitosol\\_300-TM.pdf](https://www.viessmann.de/content/dam/public-brands/master/products/solar/vitosol-300-tm/DB-5793172_Vitosol_300-TM.pdf/_jcr_content/renditions/original.media_file.download_attachment.file/DB-5793172_Vitosol_300-TM.pdf) (accessed 05/01/2023).
- [9] NARVA Lichtquellen GmbH + Co. KG, 2015. Eigensichere HEATPIPE-Vakuumröhre Temperaturbegrenzung nach dem NARVA-Prinzip. [https://www.narva-bel.de/wp-content/uploads/2021/05/flyer\\_vakuumroehren\\_eigensichere\\_heatpipe\\_narva.pdf](https://www.narva-bel.de/wp-content/uploads/2021/05/flyer_vakuumroehren_eigensichere_heatpipe_narva.pdf) (accessed 05/01/2023).
- [10] B. Schiebler, F. Weiland, F. Giovannetti, O. Kastner, S. Jack, Improved flat plate collector with heat pipes for overheating prevention in solar thermal systems, in: *Conference Proceedings, SHC/SWC Conference, Santiago, Chile, 04.-07. November 2019, 2019.*
- [11] Philippen D., Caflich M., Brunold S., Haller M., 2016. ReSoTech 1 – Reduktion der Marktpreise solarthermischer Anlagen durch neue technologische Ansätze, Teil 1: Potenzialanalyse und Lösungsansätze, Final Report, SI/501397-01.
- [12] Philippen D., Zenhäusern D., Voiron A., Dudita M., Haberl R., Lauenberger L., Thien Hui Ying V., Lebbay Maricar S.M., Haller M., Brunold S., 2020. ReSoTech 2 – Reduktion der Marktpreise solarthermischer Anlagen durch neue technologische Ansätze Teil 2, Final Report, SI/501397-02.

- [13] DIN CERTCO, 2016. Solar KEYMARK Certificate, Licence Number 011-7S2187 F.
- [14] DIN CERTCO, 2020. Solar KEYMARK Certificate, Licence Number 011-7S2994 R.
- [15] J. Jensen, B. Schiebler, F. Giovannetti, A TRNSYS type for the simulation of temperature limiting heat pipe collectors, EuroSun-Conference, Kassel, 25.-29. September 2022, 2022 (in press).
- [16] NMC-Insulation, 2022. Technische Information Anschluss technik für Solarthermie, [https://nmc-insulation.com/wp-content/uploads/sites/3/2018/06/Aeroline-SOLAR\\_DE.pdf](https://nmc-insulation.com/wp-content/uploads/sites/3/2018/06/Aeroline-SOLAR_DE.pdf) (accessed 03/02/2022).
- [17] Technische Information alpeXfränkische Rohrwerke Gebr. Kirchner GmbH & Co. KG, 2022 <https://oxomi.com/p/3000470/catalog/10046645> (accessed 03/02/2022).
- [18] PAW GmbH & Co. KG, 2020. Installation and Operation Instructions Solar stations SolarBloC midi Basic – DN 20, <https://www.paw.eu/de/amfile/file/download/file/4626/product/16151/> (accessed 05/01/2023).
- [19] PAW GmbH & Co. KG, 2014. Montage- und Bedienungsanleitung Solarstationen SolarBloC mini DN 15.
- [20] Deutsches Institut für Normung e.V. DIN EN 12828:2014, Heizungsanlagen in Gebäuden - Planung Von Warmwasser-Heizungsanlagen, Beuth Verlag, Berlin, 2014.
- [21] Verein Deutscher Ingenieure e.V. Druckhaltung, Entlüftung, Entgasung. VDI-Richtlinie 4708 Blatt 1, Beuth Verlag, Düsseldorf, 2012.
- [22] Deutsches Institut für Normung, Normenausschuss Heiz- und Raumlufttechnik (NHRS), 2018. DIN 12977-1:2018, Thermische Solaranlagen und ihre Bauteile – Kundenspezifisch gefertigte Anlagen – Teil 1: Allgemeine Anforderungen an Solaranlagen zur Trinkwassererwärmung und solare Kombianlagen.
- [23] Verein Deutscher Ingenieure e.V., Solare Trinkwassererwärmung, Allgemeine Grundlagen, Systemtechnik und Anwendung im Wohnungsbau. VDI-Richtlinie (2012) 6002 Blatt 1.
- [24] Viessmann Werke GmbH & Co. KG, 2008. Planungshandbuch Solarthermie, Allendorf.
- [25] Reflex Winkelmann GmbH, 2019. Fachgerecht planen, berechnen und ausrüsten. – Kompaktes Fachwissen für Druckhalte-, Entgasungs-, Nachspeise- und Wasseraufbereitungssysteme.
- [26] ISO 9459-5 System Performance Characterization By Means of Whole-System Tests and Computer Simulation, Beuth Verlag, Berlin, 2007.
- [27] KBB Kollektorbau GmbH, 2014. Technische Daten Flachkollektor K423DH, [https://kbb-solar.com/wp-content/uploads/2017/03/TechnDaten\\_K423DH-1.pdf](https://kbb-solar.com/wp-content/uploads/2017/03/TechnDaten_K423DH-1.pdf) (accessed 06/01/2023).
- [28] Kamstrup, 2020. Data sheet MULTICAL 603.
- [29] J. Scheuren, Untersuchungen Zum Stagnationsverhalten solarthermischer Kollektorfelder. Dissertation, Kassel University Press, 2008.
- [30] Weiss W., Spörk-Dür M., 2022. Global Market Development and Trends in 2021, Detailed Market Figures 2020. Solar Heat Worldwide. <https://www.iea-shc.org/Data/Sites/1/publications/Solar-Heat-Worldwide-2022.pdf>.
- [31] Bachmann S., Fischer S., Hafner B., 2018a. Definition of the reference solar domestic hot water (SDHW) system, Germany - Info Sheet A08, IEA TASK54. <https://task54.iea-shc.org/Data/Sites/1/publications/A08-Info-Sheet-Ref-SF-SDHW-System-Germany.pdf> (accessed 14/07/2022).
- [32] Bachmann S., Fischer S., Hafner B., 2018b. Definition of reference solar combi system for single-family house, Germany - Info Sheet A09, IEA TASK54, <https://task54.iea-shc.org/Data/Sites/1/publications/A09-Info-Sheet-Ref-SF-Solar-Combisystem-Germany.pdf> (accessed 14/07/2022).
- [33] Helbig S., Mercker O., Giovannetti, F., 2018. Definition of reference solar combi system for multifamily houses (MFH), Germany - Info Sheet A10, IEA TASK54, <https://task54.iea-shc.org/Data/Sites/1/publications/A10-Info-Sheet-Ref-MF-Solar-Combisystem-Germany.pdf> (accessed 14/07/2022).
- [34] Louvet Y., Fischer S., Furbo S., Giovannetti F., Köhl M., Mauthner F., Mugnier D., Philippen D., Veynandt F., 2019. Guideline for levelized cost of heat (LCOH) calculations for solar thermal applications. IEA TASK 54 Info Sheet A01. <https://task54.iea-shc.org/Data/Sites/1/publications/A01-Info-Sheet-LCOH-for-Solar-Thermal-Applications.pdf> (accessed 18/07/2022).
- [35] Remund J., Müller S., Schmutz M., and Graf P. Meteororm Version 8, EUPVSEC 2020 Online conference 07. - 11. September 2020.
- [36] Schiebler B., Giovannetti F., Schaffrath W., 2018b. Kostengünstige und zuverlässige Solarsysteme durch neuartige Wärmerohr-Kollektoren. Final Report, reference number 0325550A-C, [https://isfh.de/wp-content/uploads/2019/08/BMWi\\_Fkz0325550A-C\\_Abschlussbericht\\_HP-Koll.pdf](https://isfh.de/wp-content/uploads/2019/08/BMWi_Fkz0325550A-C_Abschlussbericht_HP-Koll.pdf) (accessed 18/07/2022).
- [37] B. Schiebler, F. Giovannetti, S. Fischer, Levelized Cost of Heat for Solar Thermal Systems with Overheating Prevention - Info Sheet B05, IEA SHC (2018) TASK54 <https://task54.iea-shc.org/Data/Sites/1/publications/B05-Info-Sheet-LCOH-for-Solar-Thermal-Systems-with-Overheating-Prevention.pdf>. (accessed 18/07/2022).
- [38] B. Schiebler, F. Giovannetti, S. Fischer, Reduction of Maintenance Costs by Preventing Overheating - Info Sheet B03, IEA SHC TASK54 (2018) <https://task54.iea-shc.org/Data/Sites/1/publications/B03-Info-Sheet-Reduction-of-Maintenance-Costs-by-Preventing-Overheating.pdf>. (accessed 21/07/2022).